Available online at www.sciencedirect.com
ScienceDirect
Vision Research 47 (2007) 363–374
Vision Research
www.elsevier.com/locate/visres

Visual cycle and its metabolic support in gecko photoreceptors

A.V. Kolesnikov [a,1], P. Ala-Laurila [b,1], S.A. Shukolyukov [a], R.K. Crouch [c], B. Wiggert [d], M.E. Estevez [b], V.I. Govardovskii [a,*], M.C. Cornwall [b]

[a] *Institute for Evolutionary Physiology and Biochemistry, Russian Academy of Sciences, St. Petersburg, Russia*
[b] *Department of Physiology and Biophysics, Boston University School of Medicine, Boston, MA, USA*
[c] *Department of Ophthalmology, Medical University of South Carolina, Charleston, SC, USA*
[d] *National Eye Institute, National Institutes of Health, Bethesda, MD 20892, USA*

Received 5 July 2006; received in revised form 15 August 2006

Abstract

Photoreceptors of nocturnal geckos are transmuted cones that acquired rod morphological and physiological properties but retained cone-type phototransduction proteins. We have used microspectrophotometry and microfluorometry of solitary isolated green-sensitive photoreceptors of Tokay gecko to study the initial stages of the visual cycle within these cells. These stages are the photolysis of the visual pigment, the reduction of all-*trans* retinal to all-*trans* retinol, and the clearance of all-*trans* retinol from the outer segment (OS) into the interphotoreceptor space. We show that the rates of decay of metaproducts (all-*trans* retinal release) and retinal-to-retinol reduction are intermediate between those of typical rods and cones. Clearance of retinol from the OS proceeds at a rate that is typical of rods and is greatly accelerated by exposure to interphotoreceptor retinoid-binding protein, IRBP. The rate of retinal release from metaproducts is independent of the position within the OS, while its conversion to retinol is strongly spatially non-uniform, being the fastest at the OS base and slowest at the tip. This spatial gradient of retinol production is abolished by dialysis of saponin-permeabilized OSs with exogenous NADPH or substrates for its production by the hexose monophosphate pathway (NADP + glucose-6-phosphate or 6-phosphogluconate, glucose-6-phosphate alone). Following dialysis by these agents, retinol production is accelerated by several-fold compared to the fastest rates observed in intact cells in standard Ringer solution. We propose that the speed of retinol production is set by the availability of NADPH which in turn depends on ATP supply within the outer segment. We also suggest that principal source of this ATP is from mitochondria located within the ellipsoid region of the inner segment.

Keywords: Visual cycle; Visual pigments; Gecko; Photoreceptors; Retinal; Retinol

1. Introduction

The visual cycle is a series of reactions whereby photoreceptors restore the ''dark'' state of their visual pigment after photoactivation (bleaching). These reactions subserve retinal dark adaptation, and their impairment results in the genesis of a number of retinal diseases (for recent reviews see McBee, Palczewski, Baehr, & Pepperberg, 2001; Kuksa, Imanishi, Batten, Palczewski, & Moise, 2003; Thompson & Gal, 2003; Lamb & Pugh, 2004). The initial steps of the vertebrate visual cycle occur within outer segments (OSs) of photoreceptors. They include (1) the slow photolysis reactions of meta-intermediates that decay into free all-*trans* retinal and opsin; (2) the reduction of released all-*trans* retinal to all-*trans* retinol by NADPH-dependent retinol dehydrogenase (RDH); and (3) the translocation of all-*trans* retinol from photoreceptors to the extracellular matrix. All-*trans* retinol is subsequently converted back to the 11-*cis* form in the retinal pigment epithelium cells (for rods) or possibly in Müller cells (for cones) and is then returned to the outer segments to restore ''dark'' pigment.

Recently we have found that one of the key reactions of the visual cycle, the conversion of all-*trans* retinal to all-*trans* retinol, proceeds at different speeds in different locations

* Corresponding author. Fax: +7 812 552 3012.
E-mail address: vgov@mailbox.alkor.ru (V.I. Govardovskii).
[1] The two authors contributed equally to this work.

0042-6989/$ - see front matter © 2006 Elsevier Ltd. All rights reserved.
doi:10.1016/j.visres.2006.08.024

within the outer segment, being the fastest at the OS base, and slowest at the tip, both in rods and cones (Tsina et al., 2004; Ala-Laurila et al., 2006). On the other hand, the decay of metaproducts that releases all-*trans* retinal, the substrate for the RDH reaction, occurs at the same rate throughout the OS and thus appears not to be position-dependent. These data demonstrate that the different rates of retinol production that have been observed in different regions of the OS do not arise from differential rates of metaproducts decay, but rather from other factors related to the RDH reaction itself. We hypothesized that the regional differences in the rate of retinol production within the same cell are caused by the limited local supply of the RDH cofactor NADPH. The possibility that the speed of the visual cycle in normal conditions depends on its metabolic support may have an important implication for understanding disease-related mechanisms that impair visual function.

Photoreceptors of geckos provide a particularly good model for studying the factors that control the reaction of the visual cycle within the outer segments. We will show here, as in other rods we have studied, that metaproducts decay rate following bleaching is uniform throughout the OS. However, the spatial gradient of retinol production within gecko OSs is unusually prominent, and results from a very large differential of the retinal-to-retinol reduction rate between the proximal and distal regions of the outer segment. Given these large differences, experimental perturbations of these rates are easy to measure.

These receptors have other unusual properties as well. They occupy an intermediate position between true rods and cones (Walls, 1942; Underwood, 1970; Crescitelli, 1977, 1991). As such, they appear to be transmuted cones that acquired rod morphological (Pedler & Tilly, 1964; Tansley, 1964; Röll, 2000) and physiological (Kleinschmidt & Dowling, 1975; Bodoia & Detwiler, 1985) properties but retained visual pigments and other phototransduction proteins that still can be classified as cone-like (Kojima et al., 1992; Rispoli, Sather, & Detwiler, 1993; Zhang, Wensel, & Yuan, 2006).

Previous work has demonstrated that all of the initial reactions of the visual cycle within the photoreceptor outer segment (the decay of metaproducts into retinal and opsin, enzymatic retinol production and clearance) proceed substantially faster in cones as compared to rods (Golobokova & Govardovskii, 2006; Ala-Laurila et al., 2006). These results are in a good agreement with a host of physiological and psychophysical findings showing that cones recover their sensitivity following massive bleaches about an order of magnitude faster than do rods of the same species (Jones, Crouch, Wiggert, Cornwall, & Chader, 1989; Jones, Fein, MacNichol, & Cornwall, 1993; Thomas & Lamb, 1999; Mahroo & Lamb, 2004). Thus, the more rapid operation of the visual cycle in cone photoreceptors provides the prerequisite conditions for the rapid rate of dark adaptation of diurnal vision. The study of gecko photoreceptors, which contain cone-like biochemical machinery but operate as rods, may allow clarification of the extent to which the properties of the visual cycle in different cell types stem from the evolutionary ancestry of corresponding proteins, or can/should be adapted (transmuted) to support the new function.

The goals of the experiments we report here were to use microspectrophotometric and microfluorometric measurements on intact, isolated green photoreceptors of Tokay gecko to characterize the time courses of metaproducts decay, production of all-*trans* retinol and its clearance from the cells at different locations within their outer segments. We wished to study the effects of the RDH co-factor, NADPH, and substrates involved in its generation on the rate of retinal-to-retinol conversion in order to identify the mechanism(s) that control the speed of this reaction. Secondly, we set out to determine to what extent the visual cycle of these transmuted cone receptors, which have retained cone-type pigment but rod-type physiological function, has evolved to maintain nocturnal vision in these animals.

2. Materials and methods

2.1. Animals and preparation

Experiments were performed on solitary green-sensitive photoreceptors of nocturnal gecko (*Gekko gekko*). Geckos were obtained from LA Reptiles (Los Angeles, CA) or a local pet shop (St. Petersburg, Russia) and kept at *ca.* 30 °C in heated terrariums on a 12-h light/12-h dark cycle. Animals were fed live crickets or cockroaches.

Prior to each experiment geckos were dark-adapted overnight at room temperature. Animals were decapitated in darkness and the head and body pithed. Following gross dissection of the eye, intact isolated photoreceptors were obtained by gentle shaking and teasing of small pieces dark-adapted retina in physiological solution under infrared illumination, as described previously (Cornwall, Fein, & MacNichol, 1990; Tsina et al., 2004). All procedures were performed according to protocols approved by the Animal Care and Use Committee of Boston University School of Medicine and in accordance with the standards set forth in the Guide for the Care and Use of Laboratory Animals and the Animal Welfare Act.

2.2. Solutions

The basic Ringer solution used for retina dissection and superfusion of intact isolated gecko cells was similar to that used in previous electrophysiological studies on gecko rods (Bodoia & Detwiler, 1985) and had the following composition (in mM): 159 NaCl, 3.3 KCl, 1.0 $CaCl_2$, 1.0 $MgSO_4$, 10 dextrose, 5 HEPES, pH 7.8. The solution also contained 1.5 μM bovine serum albumin. In the experiments where the effect of interphotoreceptor retinoid binding protein (IRBP) was tested, 100 μM IRBP was added directly to the solution. Experiments with exogenous NADPH or substrates for its production (glucose-6-phosphate, 6-phosphogluconate and NADP) were carried out on permeabilized outer segments (OSs). Permeabilization was achieved by adding to the perfusion solution a freshly prepared aqueous solution of saponin (1 mg/ml), to obtain a final detergent concentration of 20 μg/ml. Final concentrations of the substances were (in mM): 0.4 NADPH, 5 glucose-6-phosphate, 5 6-phosphogluconate, 0.04 NADP. Experiments were conducted at 19–22 °C.

2.3. Microspectrophotometric analysis of photolysis and retinol production

The time courses of photolysis of gecko visual pigment and retinol generation were studied with a high-speed dichroic microspectrophotometer (MSP) described earlier (Govardovskii & Zueva, 2000; Kolesnikov,

Golobokova, & Govardovskii, 2003). The MSP instrument was equipped with a computer-controlled jumping beam mask and allowed fast sequential recordings from tip and base of the same OS.

Measurements were performed on intact isolated photoreceptors or their isolated OSs in a drop of physiological solution (100–150 μl) that was placed to a superfusion chamber, the bottom of which was made of a microscope cover slip. The chamber was then located on the stage of the microspectrophotometer. Absorbance spectra were recorded at two slit positions and measuring beam polarizations (T, transversal with respect to the OS axis, and L, along the axis), in darkness and at predetermined time intervals after fast bleaching of the visual pigment. Values of absorbances at three wavelengths and two polarizations allowed determining concentrations of all six long-lived photoproducts present after bleach (metarhodopsin I, II and III (MI, MII, MIII), free all-*trans* retinal (RAL), non-specific protonated Schiff bases of retinal (PSBs), and all-*trans* retinol (ROL)). Principles of the analysis as well as its details have been described previously (Kolesnikov et al., 2003; Golobokova & Govardovskii, 2006; Ala-Laurila et al., 2006).

2.4. Microfluorometric analysis of retinol generation

The time course of postbleach retinol production within OSs of gecko green photoreceptors as well as retinol clearance from OSs was analyzed by measuring all-*trans* retinol fluorescence (Liebman, 1969; Tsina et al., 2004) using a highly sensitive microscopic fluorescent imaging system (for detailed description of the system see Tsina et al., 2004; Ala-Laurila et al., 2006). Measurements were done on solitary isolated photoreceptors continuously superfused with Ringer solution.

2.5. Light stimulation and pigment bleaching

The light stimulation procedure and the method for calculation of the bleached fraction of the visual pigment have been described previously (Tsina et al., 2004; Ala-Laurila et al., 2006). In all fluorescence experiments, we used 520 nm light for bleaching the visual pigment. The light intensities and exposure times used were calculated to produce a > 90% bleach.

2.6. Identification of cell types in microfluorometric measurements

Three kinds of visual pigments have been identified in the gecko retina. The dominant pigment has an absorption maximum at 521 nm (P521); two minor pigments have also been identified that absorb maximally at 467 nm (P467) and 364 nm (P364) (Crescitelli, Dartnall, & Loew, 1977; Loew, 1994). All three pigments are cone-like (Kojima et al., 1992; Taniguchi, Hisatomi, Yoshida, & Tokunaga, 1999; Yokoyama & Blow, 2001). To determine the spectral properties of the pigments contained within the OSs of gecko rods of the type used for microfluorometric recordings we made single-cell microspectrophotometric (MSP) measurements of their visual pigment spectra. These measurements were made using a microspectrophotometer in the Boston laboratory (MacNichol, 1978; Cornwall, MacNichol, & Fein, 1984) on samples of cells obtained from the same eyes as those from which microfluorometric experiments were made. Among the total of 57 single rods studied by this technique, 56 spectra were best-fitted by a vitamin A1 based pigment template (Govardovskii, Fyhrquist, Reuter, Kuzmin, & Donner, 2000) with a λ_{max} between 517 and 521 nm. Only one cell was blue-sensitive ($\lambda_{max} = 467$) nm. This is in fairly good agreement with the pigment distribution of gecko rods reported previously (Crescitelli et al., 1977; Loew, Govardovskii, Röhlich, & Szel, 1996). Thus, based on the overwhelming abundance of P521-containing cells in the gecko retina, we conclude that our microfluorometric measurements of retinol kinetics reflect the properties of the same dominant green-sensitive photoreceptors that were studied by MSP in St. Petersburg.

2.7. Analysis of fluorescence images

The fluorescence intensity was calculated in different regions of the gecko green photoreceptors and corrected for prebleach background fluorescence, as described earlier (Tsina et al., 2004; Ala-Laurila et al., 2006). The analyses of fluorescence images as well as the production of pseudocolor images of retinol fluorescence were carried out using Openlab 3.1 software (Improvision, Inc, MA) and Origin 6.1 (OriginLab Co., MA).

3. Results

3.1. MSP measurements of metarhodopsin decay (retinal release) in gecko green photoreceptors

The decay of metarhodopsins during photolysis is an important step in quenching of the phototransduction cascade (Leibrock, Reuter, & Lamb, 1994; Leibrock & Lamb, 1997; Leibrock, Reuter, & Lamb, 1998; Firsov, Kolesnikov, Golobokova, & Govardovskii, 2005). This decay also results in the release of all-*trans* retinal, which is reduced to all-*trans* retinol by RDH. Our previous study has shown that the rate of retinol production is grossly different among different types of salamander photoreceptors (red rods, green rods, red- and blue-sensitive cones), and even within the different regions of the same outer segment. It was fastest in the most proximal part of the outer segment, closest to cell ellipsoid, and slowest at the tip of the outer segment (Tsina et al., 2004; Ala-Laurila et al., 2006). We demonstrated that this wave-like spread of the retinol production along photoreceptors is due to differences in the speed of retinal reduction, rather than to different rates of retinal release. To test whether it is also true for gecko rods, we measured the kinetics of decay of metaproducts with two-position MSP recordings from these cells.

Fig. 1 shows the absorbance spectra recorded with T and L polarizations (see Methods) at the base and tip of gecko green photoreceptors. Recordings from the tip are shown by blue lines; measurements at the base are indicated by red lines. The spectra are normalized to unity at the spectral maximum of the dark pigment. It is apparent from these spectra that immediately after the bleaching exposure, the main peak of the pigment disappears and a mixture of Meta I (shoulder near 475 nm) and Meta II (peak at ~380 nm) is generated. This is best seen in T-polarization spectra (the curves labeled 2 s in Fig. 1A). The further progressive decrease of the magnitude of the 380-nm peak is the evidence for Meta I + II decay. The decay is not accompanied with a significant increase of the absorbance at 475 nm indicating that Meta III is only a minor photolysis intermediate in gecko green rods (curves labeled 32 s). This is clearly in contrast to the situation in amphibian red rods where Meta III is generated in a greater amount, and the rate of its production and decay contributes substantially to the total rate of retinal release (Kolesnikov et al., 2003; Ala-Laurila et al., 2006).

Further changes in the absorbance spectra demonstrate a gradual conversion of retinal to retinol. This is seen from the loss of absorbance in the 425–550 nm region of the spectrum and the appearance of the sharp peak below 340 nm (curves at 200 s, base in Fig. 1B, D). Reduction of retinal to retinol at the tip of the OS proceeds substantially slower than at its base. At 200 s postbleach,

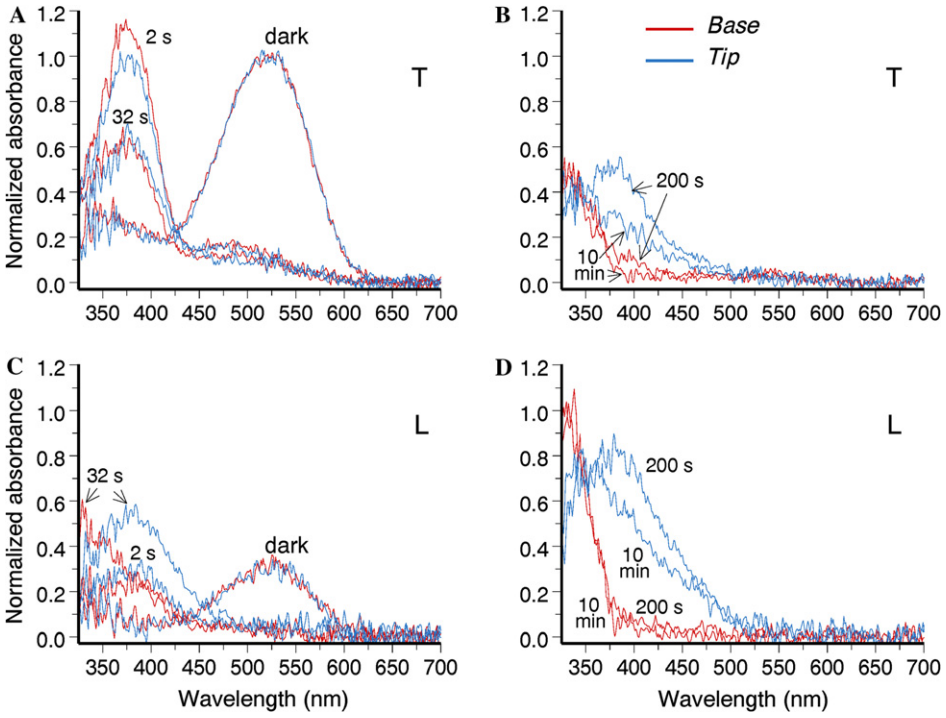

Fig. 1. Measurement of the photolysis of gecko green visual pigment in intact solitary photoreceptors by MSP. A series of spectra recorded from gecko rods at two polarizations and two positions within the OS is shown. Here and in Fig. 5, absorbance spectra recorded at the OS tip are shown by blue lines, and at the OS base, by red lines. (A) Absorbance spectra recorded at *T*-polarization in darkness and at various times after exposure to bleaching light (1500-ms flash, 525-nm). (B) same as A, at later times. C and D – same as A and B but at *L*-polarization. The spectra are normalized to unity at the T spectral maximum of the bleached pigment at each location. Recordings at 10, 100, 300 s, 15, 20, 25, 30 and 40 min are omitted from the figure for clarity. Average of two cells exhibiting fastest retinal-to-retinol conversion.

long-wavelength-absorbing substances (retinal and its PSBs) are present in significantly higher concentrations at the tip, and their conversion to retinol is incomplete even at 10 min (Fig. 1 D, blue curves).

We made two-position, two-polarization MSP measurements on more than twenty cells and always observed the base-to-tip retinol gradient. However, there was a large amount scatter in the absolute rate of retinal-to-retinol conversion among the cells. Thus, for further analysis we choose two cells that exhibited fastest rates of retinol production at the OS base. The spectra shown in Fig. 1 are averages obtained from these cells. As explained in Methods, measurements at two polarizations and three wavelengths allow determining the time courses of concentrations of all main products (MI + II, MIII, RAL, ROL, and PSB). Fig. 2 illustrates the result of such calculations based on the two selected cells. Here and throughout, concentrations of all products are normalized with respect to the concentration of bleached visual pigment.

It is apparent that the decays of metaproducts (retinal release) at the tip and base of the OS follow identical time courses (Fig. 2, closed and empty circles). By examining other cells with greatly varying rate of retinal-to-retinol conversion we found that the decay of metaproducts is independent of this rate and always follows the same time course at the tip and base. This decay can be approximated

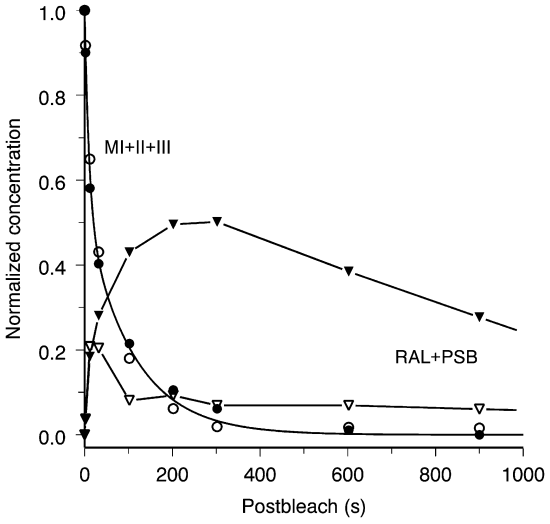

Fig. 2. Time courses of decay of the sum of metapigments (MI + II + III, circles) as well as generation of retinal and its PSB (triangles) at the tip (closed symbols) and base (empty symbols) of the OS. Smooth line shows a two-exponential approximation of pooled base and tip data on metapigments decay. Average of two "fastest" cells shown in Fig. 1.

by a bi-exponential function; the half-decay time was calculated to be 20 s. On the other hand, retinal and its PSB only transiently accumulate at the OS base (Fig. 2, open triangles), while at the tip they reach a higher concentration and persist longer (Fig. 2, closed triangles). The difference

in the time courses of the oxidized products at the two locations indicates that RAL-to-ROL reduction proceeds substantially faster at the base compared to the tip.

3.2. Microfluorometric and MSP analysis of retinol production in bleached gecko green photoreceptors

MSP measurements only provide data on the ROL time courses at two positions within the same OS. To obtain more detailed information on the spatial distribution of all-*trans* retinol and kinetics of its generation and clearance in different regions of bleached gecko cells, we performed microfluorometric measurements of intrinsic retinol fluorescence. Measurements of this kind are illustrated in the columns of pseudocolor images displayed in Fig. 3A.

At the top of the first column is a bright-field image of an isolated gecko green rod; the inner segment (IS) of the cell is on the left side and the outer segment (OS) on the right. Following this panel is a sequence of pseudocolor fluorescence images of the same cell. The first fluorescence image was taken before exposure to bright bleaching light; the other fluorescent images were measured at the indicated times following exposure to a bright bleaching light. Fluorescence intensities are coded by different colors, blue corresponding to the lowest intensity, and red to the highest intensity. Together, these images show that retinol fluorescence first increased in the most proximal part of OS, after which it slowly spread over the entire length of the OS. After reaching its maximum, ROL fluorescence slowly decreased as retinol was cleared from the cell. The results are qualitatively similar to those observed previously in bleached frog rods (Liebman, 1969; Chen et al., 2005) and all types of salamander photoreceptors (Tsina et al., 2004; Ala-Laurila et al., 2006). However, in gecko "rods" the wave-like spatial spread of retinol fluorescence along the OS was especially conspicuous, as compared to that observed earlier in all types of amphibian photoreceptor. Similar to the MSP measurements, microfluorimetry revealed base-to-tip gradients of retinol production in all cells studied, although the absolute rates at the two locations varied by as much as an order of magnitude. Also, inspection of recordings from individual cells has shown that there is only a weak correlation between the rates of retinol production between base and tip within the same OS. That is, two cells demonstrating virtually identical time courses of fluorescence at the OS base may be grossly different with respect to the fluorescence changes at the tip.

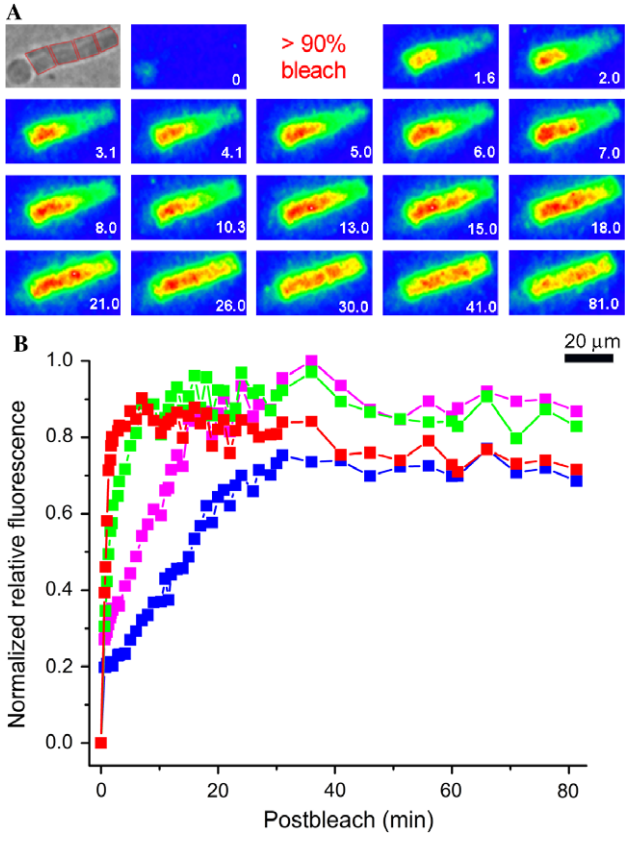

Fig. 3. (A) A bright field image of a single gecko green photoreceptor followed by a sequence of fluorescence images before and after bleaching (>90%) the visual pigment. The post-bleach time (minutes) of each fluorescence image is shown at the bottom of the image. (B) The fluorescence change of the same gecko rod analyzed in four different OS regions of similar longitudinal size outlined by red color in the bright field image shown in panel (A): red symbols (proximal OS), green symbols (mid-proximal OS), purple symbols (mid-distal OS), blue symbols (distal OS). Each curve is normalized with respect to the maximum fluorescence value in this cell (achieved at 36 min postbleach in mid-distal portion of the OS). Panel B shows all the data points obtained in the recording.

Fig. 3B shows corresponding time courses of changes in the normalized relative levels of retinol fluorescence at four locations within the OS of the cell: proximal OS (red), mid-proximal OS (green), mid-distal OS (purple) and distal OS (blue). These levels were measured in the regions of the OS that are outlined in red in the bright field image of the cell in panel A.

To compare MSP and fluorescence data, the latter should be properly scaled, since fluorescence has no intrinsic standard that allows estimation of concentration. Scaling was performed in two steps. First, the fluorescence readings for each cell were normalized with respect to the peak value reached at the OS base. Then data for all cells were averaged and scaled (using the same factor in the tip and base) for the best visual fit to the MSP data. After this processing, retinol time courses assessed by MSP and fluorescence coincided within one standard deviation (data not shown). However, such a comparison is not very informative because SD values are quite large, reaching 35%. Therefore, for more accurate comparison we choose two cells from each data set that exhibited the fastest ROL concentration/fluorescence increase at the OS base.

Fig. 4 compares the time course of retinol production at the base and tip of the OSs as measured by microspectrophotometry and microfluorometry. Retinol concentration increased much more rapidly and to a greater extent at the base of the OS (filled squares, microfluorimetry; empty squares, MSP) compared to the tip (corresponding circles). The correspondence between the two data sets is quite good at base of photoreceptor OSs. As for the tip, the

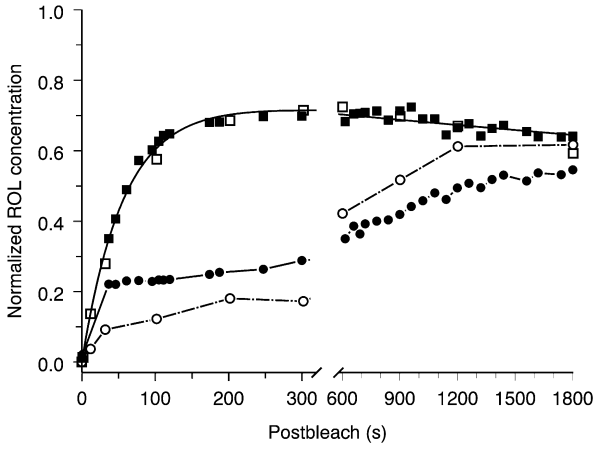

Fig. 4. Time course of retinol concentrations at the tip (circles) and base (squares) of the OSs. Empty symbols, MSP measurements, based on averaged data from two cells shown in Figs. 1, 2. Closed symbols, fluorometric measurements, show results from two cells having the fastest rates of retinol production. Fluorescence data are scaled, by the same factor for tip and base, for best visual match to MSP. Smooth line is a bi-exponential approximation of the pooled MSP and fluorometric data at the OS base. The fitted line has no mechanistic meaning and is drawn only to visually connect the data points.

correspondence is less good, though both methods show that the total rise over the 30 min of the measurement was slower and the total increase was less at the OS tip compared to its base. This discrepancy between the MSP and fluorescence at the OS tips arises from the large scatter of ROL time courses at this location, as mentioned above. Nevertheless, it is evident that both techniques are in general agreement and reveal a gross difference in the rate of retinol production at the tip and base of the gecko OS, in spite of the fact that there is no significant difference in the rate of generation of the retinal substrate for RDH (see Fig. 2).

Together these findings show that strong spatial non-uniformity in retinol production rate along the outer segment does not originate from differences in the rate of metarhodopsin decay but rather arises at a later enzymatic stage of retinal reduction.

3.3. Effect of exogenous NADPH and substrates for its generation on the rate of retinol production

It has been hypothesized that the reason for the non-uniform rate of retinol generation along the outer segment lies in insufficient supplies of the RDH co-factor, NADPH. NADPH availability, in turn, may depend on energy sources within mitochondria located in the inner segment (Tsina et al., 2004; Ala-Laurila et al., 2006). To test this idea we performed two-position MSP measurements of retinol production in gecko photoreceptors supplied with exogenous NADPH. To provide access to the OS interior, saponin (20 μg/ml) was added to the perfusion solution. Treatment of intact gecko photoreceptors with saponin at this concentration caused in most cases the detachment of the outer segment from the inner segment. On the other hand, lower concentrations of the detergent (up to 10–15 μg/ml) were insufficient to ensure NADPH penetration through the plasma membrane, as can be judged from unaltered kinetics of retinol production as compared to control measurements made on intact cells when no saponin or exogenous NADPH were present. Thus, all experiments of this sort were carried out on isolated outer segments. Control experiments showed, both by MSP and fluorometric recording that these OSs, whether permeabilized or untreated, were incapable of retinol production in the absence of exogenous NADPH. In order to distinguish between base and tip of the outer segment in each specific case, we used a morphological criterion. We selected only cells with a markedly larger diameter at the one end of OS, which we identified as the base of OS. The NADPH absorbance band at 340 nm does not interfere with MSP measurements because the absorption in the surrounding medium is excluded by the difference measurement routine. Similar microfluorometric measurements are not possible because the intrinsic fluorescence of NADPH in the bulk solution would completely obscure the retinol signal from the OS.

Fig. 5 illustrates a series of average absorbance spectra recorded with T and L polarizations at the tip and base of saponin-permeabilized OSs in presence of 0.4 mM NADPH. As in Fig. 1, recordings from the tip are shown by blue lines; measurements at the base are indicated by red lines. The gradient of retinol formation along OS axis is not observed in this condition as seen from identical spectra measured at both proximal and distal locations at all post-bleach times. This is in marked contrast to the widely different rates of retinol production that are observed when gecko rods are bathed in normal Ringer solution (compare with Fig. 1). The average absolute rate of retinal reduction in the case of NADPH dialysis is higher than that observed at the base of OS in normal Ringer, and the ROL-dominant shape of the spectra is established already by 5 min after bleaching of the visual pigment (Figs. 5C, D). However, it is apparent from the spectra recorded at 15 min and later that the conversion of retinal to retinol in the presence of NADPH is less complete than it is at the OS base in intact photoreceptors in normal Ringer. Changes in the absorbance spectra at later times reveal clearance of retinol from photoreceptors as evidenced by the loss of absorbance below 350 nm (Fig. 5 D). The effect of NADPH on the time courses of oxidized RDH substrates (RAL and PSB) and their reduction to retinol is illustrated in Figs. 6 A, C (triangles).

The results show that the non-uniform pattern of retinol production in OS of gecko photoreceptors in normal physiological conditions arises from a deficiency in the NADPH supply at the distal part of the OSs rather than from a difference in RDH enzymatic activity in this region.

To determine what factors control NADPH production under this condition we performed analogous experiments in which OSs were treated with exogenous NADP and glucose-6-phosphate (G6P) or 6-phosphogluconate (6PG)

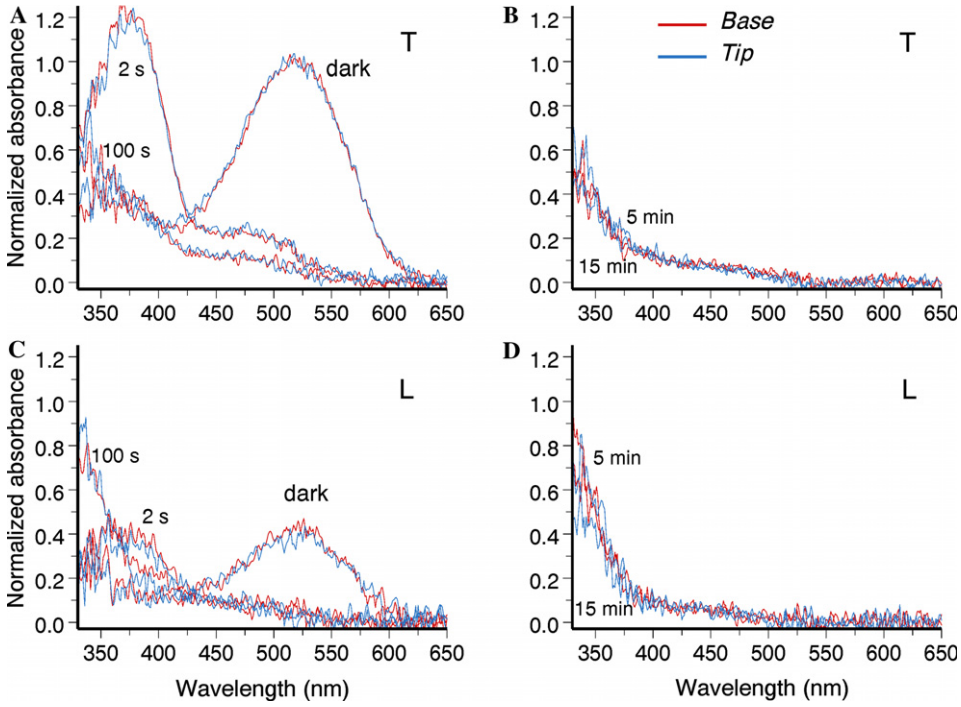

Fig. 5. Effect of dialysis of 0.4 mM NADPH on the RAL to ROL reduction at the tip and base in isolated, saponin-permeabilized outer segments. Absorbance spectra at the two locations are identical within the noise level, showing that exogenous NADPH abolishes the longitudinal gradient of retinol production. Average of 8 OSs.

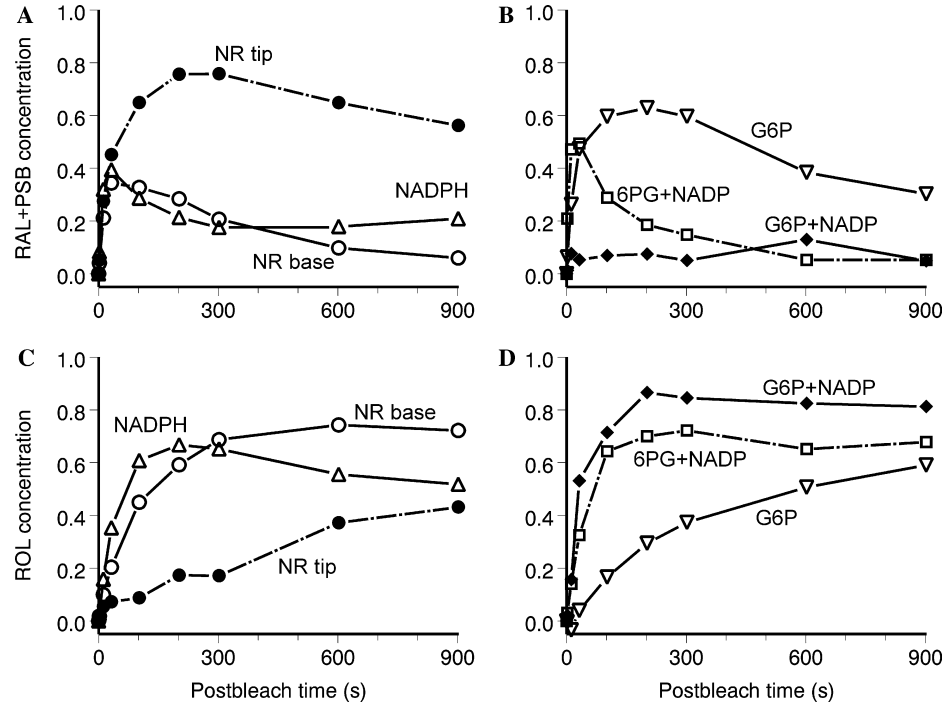

Fig. 6. Comparison of effects of various co-factors on the time courses of oxidized RDH substrates (RAL + PSB) (panels A and B) and their reduction to retinol (panels C and D) in gecko green photoreceptors. The same experimental conditions are marked with the same symbols/line styles in each pair of panels. Average of 7 cells with fastest RAL to ROL conversion (normal Ringer), 8 OSs (NADPH), 6 OSs (G6P), 8 OSs (G6P + NADP), and 5 OSs (6PG + NADP). NR: data obtained separately from the OS tip and base on intact cells in normal Ringer. All other data are from saponin-permeabilized isolated OSs and are averages of the OS tip and base because there was no difference in time courses at the two locations.

rather than NADPH. These substances are the substrates required for the production of NADPH by the hexose phosphate metabolic pathway in photoreceptors (Hsu & Molday, 1994). Production of NADPH in the pathway is catalyzed by two enzymes, glucose-6-phosphate dehydrogenase (G6P-DH) and phosphogluconate dehydrogenase (PG-DH). In agreement with the results obtained when NADPH alone was present in the medium, the rate of retinol production in 5 mM G6P and 0.04 mM NADP was identical at both the proximal and distal parts of OS. Moreover, the conversion of retinal to retinol in this case occurred faster than in NADPH-containing medium and was almost complete within 4–5 min after bleach, while RAL + PSB accumulated to substantially lower concentration (Figs. 6 B, D, diamonds). 5 mM 6PG + 0.04 mM NADP were only slightly less efficient than G6P + NADP in accelerating retinol production over entire OS length (Fig. 6 D, squares). Finally, dialysis of G6P alone (5 mM) also abolished the base-to-tip gradient of retinol production rate (Fig. 6 D, triangles). Taken together, these data indicate that NADPH production is likely limited by the availability of phosphorylated glucose and not due to a decreased intrinsic rate of the RDH activity at the tip of the OS.

3.4. Effect of IRBP on retinol clearance

Following enzymatic generation of all-*trans* retinol within photoreceptor OSs, the latter must be transferred to the extracellular space for further processing. In the rod visual cycle this takes place in the cells of retinal pigment epithelium; in the cone visual cycle this may take place in Müller cells as well (Mata, Radu, Clemmons, & Travis, 2002). Consistent with the idea, the microfluorometric and MSP measurements in standard Ringer solution both demonstrate that, after its production, retinol is slowly cleared from the outer segments (Figs. 3, 4). However, the time constant for this clearance is very long (roughly 4 h), and thus is incompatible with the normal speed of the visual cycle, either in cones or rods. It has been demonstrated previously that the clearance of retinol from all types of bleached salamander photoreceptors can be significantly facilitated by addition of interphotoreceptor retinoid binding protein (IRBP) (Tsina et al., 2004; Ala-Laurila et al., 2006). Similar results have been also obtained on toad rods by using HPLC analysis of retinoids (Qtaishat, Wiggert, & Pepperberg, 2005). This protein is the most abundant soluble protein in the interphotoreceptor matrix (Shaw & Noy, 2001; Loew & Gonzalez-Fernandez, 2002). We found that IRBP (100 μM) added to the superfusate efficiently facilitated retinol clearance from gecko photoreceptors as well (Fig. 7).

The continuous curves in the main panel represent two-exponential fits to the averaged and normalized experimental data on retinol production and clearance from proximal parts of OSs of intact gecko photoreceptors. In agreement with previous report on salamander (Tsina et al., 2004; Ala-Laurila et al., 2006), treatment with IRBP resulted in an approximately 20-fold increase in the rate of retinol transport from gecko photoreceptors (corresponding time constants are 13.6 min in the presence of IRBP, and 241 min in its absence). In addition, the absolute peak level of retinol fluorescence measured in the presence of IRBP in gecko cells (see Fig. 7, inset) was significantly lower than in its absence. Notably, these two curves initially follow the same course, and only diverge at later times. These changes in fluorescence are consistent with the idea that IRBP accelerates the clearance of retinol but has little effect on its production.

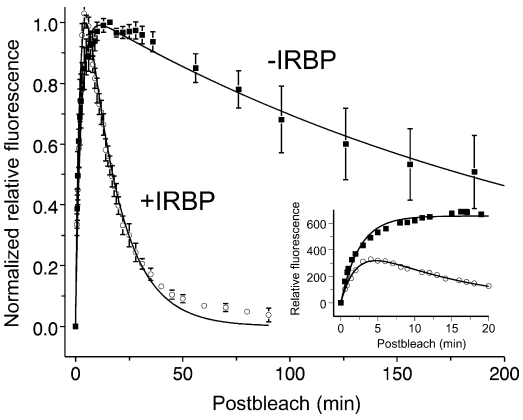

Fig. 7. Effect of IRBP on retinol accumulation and clearance in OSs of intact isolated gecko photoreceptors measured microfluorometrically. In the main panel: the average fluorescence intensities at the OS base measured in normal Ringer (squares, $n = 11$) and in the presence of 100 μM IRBP (circles, $n = 6$); each data are normalized to unity with respect to its own maximum. Error bars show SEM values. The inset plots the same data as in the main panel but data have not been normalized.

4. Discussion

4.1. Kinetics of decay of metaproducts of the gecko green visual pigment

We have characterized the kinetics of the main stages of the visual cycle that occur within the outer segments of gecko green photoreceptors. These cells contain the visual pigment that originated from an M/LWS-cone pigment of geckos' diurnal ancestors (Kojima et al., 1992; Taniguchi et al., 1999; Yokoyama & Blow, 2001). The pigment retains basic cone-like properties. It is destroyed by hydroxylamine, and its absorbance spectrum is pH- and anion-dependent (summarized in Crescitelli, 1977, 1991). However, its absorbance maximum, 521 nm, is shifted from that of typical cone iodopsin (560-570 nm) towards rod rhodopsin (near 500 nm). We found that the rate of photolysis of the gecko green pigment is also "transmuted", that is, it is substantially slowed compared to M/LWS cone pigments. The kinetics of decay of metaproducts in gecko green photoreceptors occupies an intermediate position between "genuine" LWS-pigments of red-sensitive cones of salamander or goldfish, and amphibian

or goldfish rhodopsin/porphyropsin rods (RH1-pigments) (Fig. 8). The slowness of the photolysis is apparently not caused by the short-wave shift of absorbance as such. The green-sensitive (RH2) cone visual pigment in goldfish, which is spectrally similar to gecko green, exhibits the fast photolysis kinetics virtually indistinguishable from that in goldfish LWS cones (Fig. 8; see Golobokova & Govardovskii, 2006). Thus, we believe that the retardation of photolysis in gecko green photoreceptors is an adaptation to the function at low light levels characteristic of "true" rods.

It has been hypothesized that faster photolysis of cone visual pigments is somehow linked to lower dark stability of the chromophore-to-opsin linkage that results in a high rate of spontaneous thermal activation of the pigment and persistence of a substantial fraction of "naked" (chromophore-free) opsin in dark-adapted cones (Rieke & Baylor, 2000; Kefalov et al., 2005; Golobokova & Govardovskii, 2006). Both the thermal activation in darkness and the presence of free opsin substantially desensitize cones, so the loose linkage of the chromophore to opsin may be prohibitive for high-sensitive rod-like photoreceptors. The short-wave shift of the absorbance of the gecko green pigment may be a means to stabilize its structure (e.g. by increasing the energy needed for the activation of the pigment), and could also result in higher stability/longer life times of its Meta states found in this study.

4.2. Rate of retinol production

The next stage of the visual cycle is the reduction of all-*trans* retinal to all-*trans* retinol catalyzed by retinol dehydrogenase (Futterman, 1963; Palczewski et al., 1994; Rattner, Smallwood, & Nathans, 2000). This reaction is supposed to remove retinal, which, in addition to being toxic, is capable of blocking the light-regulated channels in the plasma membrane (Dean, Nguitragool, Miri, McCabe, & Zimmerman, 2002; McCabe et al., 2004; Horrigan et al., 2005) and activates phototransduction (Kefalov, Crouch, & Cornwall, 2001) thus retarding dark adaptation. Besides, this stage provides the substrate for the restoration of the 11-*cis* retinal.

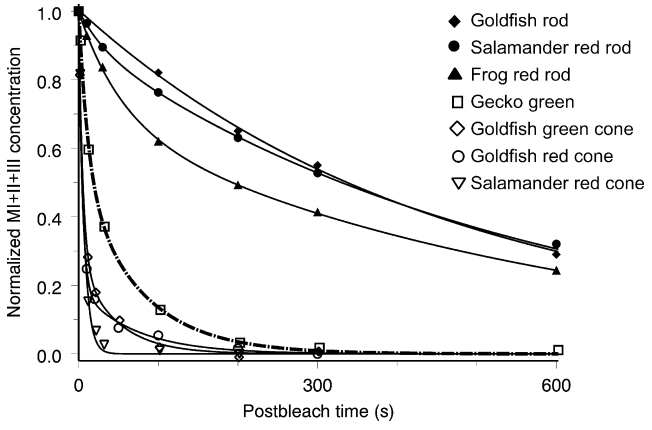

Fig. 8. Comparison of time courses of the decay of metaproducts (all-*trans* retinal release) in various types of photoreceptors. Data for salamander photoreceptors are from Ala-Laurila et al., 2006; for goldfish, from Golobokova and Govardovskii, 2006; for frog, from Kolesnikov et al., 2003.

This reaction in gecko green photoreceptors also proceeds at the rate intermediate between typical rods and cones (Fig. 9A). It is 8-times faster than in salamander red rods yet 3-4-times slower than in salamander SWS2/M/LWS cones. However, the slowness of retinol generation in gecko rods compared to cones is mostly due to the slowness of the release of all-*trans* retinal from metaproducts rather than due to intrinsic slowness of gecko's retinoldehydrogenase. V_{max} of RDH reaction in various cells can be estimated from the model of retinal-to-retinol conversion described in Ala-Laurila et al. (2006). Corresponding calculations show that the intrinsic activity of RDH in gecko green rods is more than an order of magnitude higher than in salamander red rods, and is clearly in the cone range (Fig. 9B).

4.3. Clearance of retinol from gecko photoreceptors

Transfer of all-*trans* retinol from the outer segment across the plasma membrane to the intercellular space is an important step in the visual cycle. It facilitates recovery of dark current (Jones et al., 1989) and, maybe more importantly, provides the substrate for further restoration of the 11-*cis* chromophore in pigment epithelial or Müller cells. We found that this process in gecko proceeds very slowly in normal Ringer, with the time constant of 4 hrs (Fig. 7, line trough squares). This seems incompatible with normal functioning of dark adaptation mechanisms. Like in other types of photoreceptors (Ala-Laurila et al., 2006), clearance is accelerated more than tenfold by an addition of IRBP to the bathing solution (Fig. 7, line through circles).

Interestingly, the rate of retinol clearance from gecko photoreceptors places them among rods rather than cones. The characteristic time constant of un-aided clearance of retinol from salamander red rods is ca. 5 hrs, while in cones it is between 10 and 20 min. In the presence of IRBP these time constants are reduced to 25 and 4 min, respectively (Ala-Laurila et al., 2006). We hypothesized earlier that the rate of retinol clearance is mainly controlled by the OS surface-to-volume ratio. It is substantially higher in cones than in rods due to the fact that cone disks represent essentially invaginations of the OS plasma membrane. Based on electron microscopic observations, OS disks of gecko "rods" appear to form the invaginations of the plasma membrane consistent with their cone origin (Dunn, 1966; Yoshida, 1978; Röll, 2000). However, in experiments using a membrane-impermeable fluorescent dye to probe the functional accessibility of these invaginations it has been shown that only a short stack of disks located at the base of gecko OSs has access to the extracellular space (Laties, Bok, & Liebman, 1976). Thus, gecko photoreceptors are transmuted towards rods not only with respect to their overall morphology, but also with respect to the

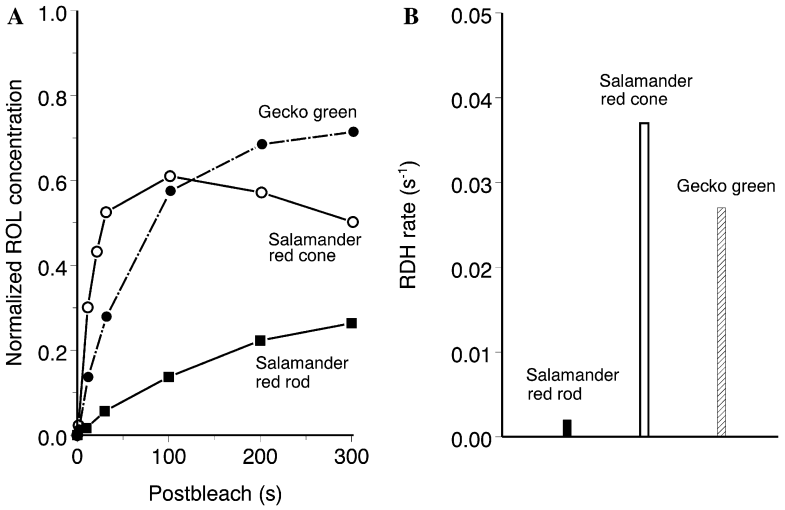

Fig. 9. Comparison of retinol production and RDH activity in various types of photoreceptors showing that gecko green "rods" group with cones accordingly to these parameters. A, time courses of retinol concentration at the OS base of intact cells in normal Ringer. B, RDH V_{max} inferred from the model that takes into account the rate of retinal release from metaproducts (Ala-Laurila et al., 2006).

surface-to-volume ratio of their OSs, with corresponding effect on the rate of exchange of retinoids with accessory cells that support the visual cycle.

The general slowness of the visual cycle in gecko green photoreceptors, compared to their cone ancestors, hardly poses any problem to this animal that is strictly nocturnal. Gecko photoreceptors are never subjected to high bleaches in the animal's natural environment. However, the gecko case is instructive because it allows a more clear examination of the processes that limit the rate of the visual cycle. This can be crucial for photoreceptors that are normally subjected to bright light, that is for cones and rods in diurnal species. Our results suggest that in normal condition the speed of the visual cycle may mostly depend on its metabolic support rather than on the rate of the visual pigment photolysis and RDH activity.

4.4. Metabolic support of the visual cycle in photoreceptors

It is shown recently that the production of retinol proceeds at different rates in various regions of the outer segment, being the fastest at the OS base, and slowest at its tip (Tsina et al., 2004; Ala-Laurila et al., 2006). This feature is the most conspicuous in gecko "rods" (Figs. 3, 4). Since there is no marked regional difference in the rate of retinal release from metaproducts (Fig. 2), the rate of retinol production is obviously dependent on the local rate of retinal-to-retinol conversion by RDH. We have hypothesized earlier that there is no difference either in intrinsic properties of RDH enzyme or its content between newly synthesized disks at the OS base and "old" disks at the tip (Ala-Laurila et al., 2006). Rather, the gradient of retinol production is due to limit in the supply of the key cofactor of the reaction, NADPH, that in turn may depend on local availability of other reduced substrates. Present experiments with addition of NADPH and substrates for its production support this hypothesis. Indeed, NADPH abolished the difference between the OS base and tip (Fig. 5) and increased the speed of the retinol production at both locations to the level higher than any observed in normal Ringer (Fig. 6 C). Thus, the supply of NADPH appears to be the main factor that sets the speed of the RDH reaction in gecko (and, probably, other) photoreceptors under normal conditions.

NADPH is produced in the OS mainly in the hexose monophosphate pathway (Hsu & Molday, 1991, 1994) (Fig. 10). The primary substrate is glucose (G) that is transferred from the extracellular space to the OS cytoplasm by a glucose transporter (GT). Glucose is converted to glucose-6-phosphate (G6P) by the first enzyme of glycolysis, hexokinase (HK) that utilizes ATP as a source of phosphate. Glucose-6-phosphate, in turn, is consumed by

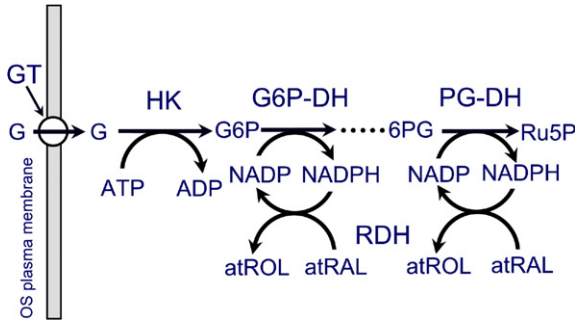

Fig. 10. A simplified scheme of NADPH production and reduction of retinal in photoreceptor outer segments based on Futterman (1963) and Hsu and Molday (1991, 1994) data. G, glucose; GT, glucose transporter; HK, hexokinase; G6P, glucose-6-phosphate, G6P-DH, glucose-6-phosphate dehydrogenase; 6PG, 6-phosphogluconate; PG-DH, phosphogluconate dehydrogenase; Ru5P, ribulose-5-phosphate; RDH, retinoldehydrogenase; atRAL, all-*trans* retinal; atROL, all-*trans* retinol. The intermediate step of generation of 6PG via 6-phosphoglucono-δ-lactone is omitted.

G6P-DH to reduce NADP to NADPH. NADPH is also produced in the second stage that uses 6-phosphogluconate to reduce NADP. The reaction is catalyzed by phosphogluconate dehydrogenase (PG-DH). NADPH is further used for reduction of retinal to retinol by RDH (Futterman, 1963; Hsu & Molday, 1994; Palczewski et al., 1994; Rattner et al., 2000). Exhaustible substrates are G and ATP; NADP is recycled. This, probably oversimplified, scheme is well supported by our results.

Thus, supplying endogenous G6P-DH with exogenous G6P and NADP results in the fastest rate of retinol production that is ca. six-fold higher than in intact cells bathed with normal Ringer containing 10 mM glucose (compare Fig. 6 C, open circles, and D, diamonds). 6PG + NADP were almost as efficient as G6P+NADP in supporting retinal reduction (Fig. 6 B, D, squares) indicating that PG-DH may also contribute to NADPH generation in the OS. The apparently counterintuitive fact that NADPH itself is less efficient than G6P + NADP can be explained by the accumulation of high concentration of NADP when NADPH is used as the substrate. NADP then acts as an inhibitor of retinal reduction (Nicotra & Livrea, 1981). With G6P + NADP added, NADP is not accumulated but recycled, so no inhibition occurs. Relatively low efficiency of G6P alone may be due to the shortage of endogenous NADP in "leaky" permeabilized OSs. In intact cells with preserved NADP pool, the limiting factor then may be the production of G6P by HK that is critically dependent on ATP supply.

Apparently, there is a significant pool of ATP, on the order of a few mM, present in dark-adapted outer segments (Carretta & Cavaggioni, 1976; Zuckerman, Schmidt, & Dacko, 1982). However, it is likely that this supply is quickly consumed after bleaching by multiple phosphorylation of rhodopsin and by other light-stimulated ATP-dependent reactions. Therefore the generation of G6P should rely on newly synthesized ATP whose main source is in the mitochondria of the inner segment. A supply of ATP diffusing from this source could result in the wave-like spread of retinol generation from the base to the tip of the OS that we observe in our experiments (Fig. 3). Similar gradient has earlier been observed for another ATP-consuming reaction, rhodopsin phosphorylation (Paulsen & Rudolphi, 1980; Paulsen & Schurhoff, 1979).

The fact that the speed of retinol production can be increased by almost an order of magnitude by adding phosphorylated glucose derivatives and co-factors (Fig. 6 C, D) suggests that under normal condition the rate of the RDH reaction is actually set by its metabolic support. Thus it may appear that the visual cycle can be impaired not only by abnormalities of participating proteins (like the visual pigment, ABCR transporter, RDH and so on), but also by disturbances of general cellular metabolism.

Acknowledgments

This work was supported by NIH Grants EY01157, EY04939, EY14850, CRDF Grant RUB1-2628 and the Russian Foundation for Basic Research Grant 06-04-48914.

References

Ala-Laurila, P., Kolesnikov, A. V., Crouch, R. K., Tsina, E., Shukolyukov, S. A., Govardovskii, V. I., et al. (2006). Visual cycle: dependence of retinol production and removal on photoproduct decay and cell morphology. *Journal of General Physiology, 128*, 153–169.

Bodoia, R. D., & Detwiler, P. B. (1985). Patch-clamp recordings of the light-sensitive dark noise in retinal rods from lizard and frog. *Journal of Physiology, 367*, 183–216.

Carretta, A., & Cavaggioni, A. (1976). On the metabolism of the rod outer segments. *Journal of Physiology, 257*, 687–697.

Chen, C., Tsina, E., Cornwall, M. C., Crouch, R. K., Vijayaraghavan, S., & Koutalos, Y. (2005). Reduction of all-*trans* retinal to all-*trans* retinol in the outer segments of frog and mouse rod photoreceptors. *Biophysical Journal, 88*, 2278–2287.

Cornwall, M. C., Fein, A., & MacNichol, E. F. Jr., (1990). Cellular mechanisms that underlie bleaching and background adaptation. *Journal of General Physiology, 96*, 345–372.

Cornwall, M. C., MacNichol, E. F., Jr., & Fein, A. (1984). Absorbance and spectral sensitivity measurements of rod photoreceptors of the tiger salamander, Ambystoma tigrinum. *Vision Research, 24*, 1561–1569.

Crescitelli, F. (1977). The visual pigments of geckos and other vertebrates: an essay in comparative biology. In F. Crescitelli (Ed.). *Handbook of sensory physiology* (Vol. 7/5, pp. 391–450). Berlin: Springer.

Crescitelli, F. (1991). The natural history of visual pigments. In N. Osborne & G. Chader (Eds.). *Progress in retinal research* (Vol. 11, pp. 1–32). Oxford: Pergamon.

Crescitelli, F., Dartnall, H. J. A., & Loew, E. R. (1977). The gecko visual pigments: a microspectrophotometric study. *Journal of Physiology, 268*, 559–573.

Dean, D. M., Nguitragool, W., Miri, A., McCabe, S. L., & Zimmerman, A. L. (2002). All-*trans*-retinal shuts down rod cyclic nucleotide-gated ion channels: a novel role for photoreceptor retinoids in the response to bright light? *Proceedings of the National Academy of Sciences of the United States of America, 99*, 8372–8377.

Dunn, R. F. (1966). Studies on the retina of the gecko *Coleonyx variegatus*. *Journal of Ultrastructure Research, 16*, 651–671.

Firsov, M. L., Kolesnikov, A. V., Golobokova, E. Y., & Govardovskii, V. I. (2005). Two realms of dark adaptation. *Vision Research, 45*, 147–151.

Futterman, S. (1963). Metabolism of the Retina. *Journal of Biological Chemistry, 238*, 1145–1150.

Golobokova, E. Y., & Govardovskii, V. I. (2006). Late stages of visual pigment photolysis *in situ*: cones vs. rods. *Vision Research, 46*, 2287–2297.

Govardovskii, V. I., Fyhrquist, N., Reuter, T., Kuzmin, D. G., & Donner, K. (2000). In search of the visual pigment template. *Visual Neuroscience, 17*, 509–528.

Govardovskii, V. I., & Zueva, L. V. (2000). Fast-recording microspectrophotometer for studying photolysis of visual pigments *in situ*. *Sensory Systems (in Russian), 14*, 288–296.

Horrigan, D. M., Tetreault, M. L., Tsomaia, N., Vasileiou, C., Borhan, B., Mierke, D. F., et al. (2005). Defining the retinoid binding site in the rod cyclic nucleotide-gated channel. *Journal of General Physiology, 126*, 453–460.

Hsu, S. C., & Molday, R. S. (1991). Glycolytic enzymes and a GLUT-1 glucose transporter in the outer segments of rod and cone photoreceptor cells. *Journal of Biological Chemistry, 266*, 21745–21752.

Hsu, S. C., & Molday, R. S. (1994). Glucose metabolism in photoreceptor outer segments. Its role in phototransduction and in NADPH-requiring reactions. *Journal of Biological Chemistry, 269*, 17954–17959.

Jones, G. J., Crouch, R. K., Wiggert, B., Cornwall, M. C., & Chader, G. J. (1989). Retinoid requirements for recovery of sensitivity after visual

pigment bleaching in isolated photoreceptors. *Proceedings of the National Academy of Sciences of the United States of America, 86*, 9606–9610.

Jones, G. J., Fein, A., MacNichol, E. F., Jr., & Cornwall, M. C. (1993). Visual pigment bleaching in isolated salamander retinal cones. Microspectrophotometry and light adaptation. *Journal of General Physiology, 102*, 483–502.

Kefalov, V. J., Crouch, R. K., & Cornwall, M. C. (2001). Role of noncovalent binding of 11-*cis*-retinal to opsin in dark adaptation of rod and cone photoreceptors. *Neuron, 29*, 749–755.

Kefalov, V. J., Estevez, M. E., Kono, M., Goletz, P. W., Crouch, R. K., Cornwall, M. C., et al. (2005). Breaking the covalent bond – a pigment property that contributes to desensitization in cones. *Neuron, 46*, 879–890.

Kleinschmidt, J., & Dowling, J. E. (1975). Intracellular recordings from gecko photoreceptors during light and dark adaptation. *Journal of General Physiology, 66*, 617–648.

Kojima, D., Okano, T., Fukada, Y., Shichida, Y., Yoshizawa, T., & Ebrey, T. G. (1992). Cone visual pigments are present in gecko rod cells. *Proceedings of the National Academy of Sciences of the United States of America, 89*, 6841–6845.

Kolesnikov, A. V., Golobokova, E. Y., & Govardovskii, V. I. (2003). The identity of metarhodopsin III. *Visual Neuroscience, 20*, 249–265.

Kuksa, V., Imanishi, Y., Batten, M., Palczewski, K., & Moise, A. R. (2003). Retinoid cycle in the vertebrate retina: experimental approaches and mechanisms of isomerization. *Vision Research, 43*, 2959–2981.

Lamb, T. D., & Pugh, E. N. Jr., (2004). Dark adaptation and the retinoid cycle of vision. *Progress in Retinal and Eye Research, 23*, 307–380.

Laties, A. M., Bok, D., & Liebman, P. (1976). Procion yellow: a marker dye for outer segment disc patency and for rod renewal. *Experimental Eye Research, 23*, 139–148.

Leibrock, C. S., & Lamb, T. D. (1997). Effect of hydroxylamine on photon-like events during dark adaptation in toad rod photoreceptors. *Journal of Physiology, 501*, 97–109.

Leibrock, C. S., Reuter, T., & Lamb, T. D. (1994). Dark adaptation of toad rod photoreceptors following small bleaches. *Vision Research, 34*, 2787–2800.

Leibrock, C. S., Reuter, T., & Lamb, T. D. (1998). Molecular basis of dark adaptation in rod photoreceptors. *Eye, 12*, 511–520.

Liebman, P. A. (1969). Microspectrophotometry of retinal cells. *Annals of New York Academy of Sciences, 157*, 250–264.

Loew, E. R. (1994). A third, ultraviolet-sensitive, visual pigment in the Tokay Gecko, *Gecko gecko*. *Vision Research, 34*, 1427–1432.

Loew, A., & Gonzalez-Fernandez, F. (2002). Crystal structure of the functional unit of interphotoreceptor retinoid binding protein. *Structure (Cambridge), 10*, 43–49.

Loew, E. R., Govardovskii, V. I., Röhlich, P., & Szel, A. (1996). Microspectrophotometric and immunocytochemical identification of ultraviolet photoreceptors in geckos. *Visual Neuroscience, 13*, 247–256.

MacNichol, E. F. Jr., (1978). A photon-counting microspectrophotometer for the study of single vertebrate photoreceptor cells. In S. J. Cool & E. L. Smith (Eds.), *Frontiers of Visual Science* (pp. 194–208). Berlin: Springer.

Mahroo, O. A., & Lamb, T. D. (2004). Recovery of the human photopic electroretinogram after bleaching exposures: estimation of pigment regeneration kinetics. *Journal of Physiology, 554*, 417–437.

Mata, N. L., Radu, R. A., Clemmons, R. C., & Travis, G. H. (2002). Isomerization and oxidation of vitamin A in cone-dominant retinas: a novel pathway for visual-pigment regeneration in daylight. *Neuron, 36*, 69–80.

McBee, J. K., Palczewski, K., Baehr, W., & Pepperberg, D. R. (2001). Confronting complexity: the interlink of phototransduction and retinoid metabolism in the vertebrate retina. *Progress in Retinal and Eye Research, 20*, 469–529.

McCabe, S. L., Pelosi, D. M., Tetreault, M., Miri, A., Nguitragool, W., Kovithvathanaphong, P., et al. (2004). All-*trans*-retinal is a closed-state inhibitor of rod cyclic nucleotide-gated ion channels. *Journal of General Physiology, 123*, 521–531.

Nicotra, C., & Livrea, M. A. (1981). Retinol dehydrogenase from bovine retinal rod outer segments. Kinetic mechanisms of the solubilized enzyme. *Journal of Biological Chemistry, 257*, 11836–11841.

Palczewski, K., Jager, S., Buczylko, J., Crouch, R. K., Bredberg, D. L., Hofmann, K. P., et al. (1994). Rod outer segment retinol dehydrogenase: substrate specificity and role in phototransduction. *Biochemistry, 33*, 13741–13750.

Paulsen, R., & Rudolphi, P. (1980). Rhodopsin phosphorylation in the frog retina: analysis by autoradiography. *Neurochemistry International, 1*, 287–297.

Paulsen, R., & Schurhoff, K. (1979). The localization of phosphorylated rhodopsin in the frog rod outer segments. *European Journal of Cell Biology, 19*, 35–39.

Pedler, C., & Tilly, R. (1964). The nature of the gecko visual cell. A light and electron microscopic study. *Vision Research, 4*, 499–510.

Qtaishat, N. M., Wiggert, B., & Pepperberg, D. R. (2005). Interphotoreceptor retinoid-binding protein (IRBP) promotes the release of all-*trans* retinol from the isolated retina following rhodopsin bleaching illumination. *Experimental Eye Research, 81*, 455–463.

Rattner, A., Smallwood, P. M., & Nathans, J. (2000). Identification and characterization of all-trans-retinol dehydrogenase from photoreceptor outer segments, the visual cycle enzyme that reduces all-*trans*-retinal to all-*trans*-retinol. *Journal of Biological Chemistry, 275*, 11034–11043.

Rieke, F., & Baylor, D. A. (2000). Origin and functional impact of dark noise in retinal cones. *Neuron, 26*, 181–186.

Rispoli, G., Sather, W. A., & Detwiler, P. B. (1993). Visual transduction in dialysed detached rod outer segments from lizard retina. *Journal of Physiology, 465*, 513–537.

Röll, B. (2000). Gecko vision – visual cells, evolution, and ecological constraints. *Journal of Neurocytology, 29*, 471–484.

Shaw, N. S., & Noy, N. (2001). Interphotoreceptor retinoid-binding protein contains three retinoid binding sites. *Experimental Eye Research, 72*, 183–190.

Taniguchi, Y., Hisatomi, O., Yoshida, M., & Tokunaga, F. (1999). Evolution of visual pigments in geckos. *FEBS Letters, 445*, 36–40.

Tansley, K. (1964). The gecko retina. *Vision Research, 4*, 33–37.

Thomas, M. M., & Lamb, T. D. (1999). Light adaptation and dark adaptation of human rod photoreceptors measured from the a-wave of the electroretinogram. *Journal of Physiology, 518*, 479–496.

Thompson, D. A., & Gal, A. (2003). Vitamin A metabolism in the retinal pigment epithelium: Genes, mutations and diseases. *Progress in Retinal and Eye Research, 22*, 683–703.

Tsina, E., Chen, C., Koutalos, Y., Ala-Laurila, P., Tsacopoulos, M., Wiggert, B., et al. (2004). Physiological and microfluorometric studies of reduction and clearance of retinal in bleached rod photoreceptors. *Journal of General Physiology, 124*, 429–443.

Underwood, G. (1970). In C. Gans & T. S. Parsons (Eds.). *The eye. Biology of the Reptilia* (Vol. 2, pp. 7–97). New York: Academic Press.

Walls, G. (1942). *The vertebrate eye and its adaptive radiation*. Bloomfield Hills: Cranbrook Institute of Science.

Yokoyama, S., & Blow, N. S. (2001). Molecular evolution of the cone visual pigments in the pure rod-retina of the nocturnal gecko, *Gekko gekko*. *Gene, 276*, 117–125.

Yoshida, M. (1978). Some observations on the patency in the outer segments of photoreceptors of the nocturnal gecko. *Vision Research, 18*, 137–143.

Zhang, X., Wensel, T. G., & Yuan, C. (2006). Tokay gecko photoreceptors achieve rod-like physiology with cone-like proteins. *Photochemistry and Photobiology*, doi: 10.1562/2006-01-05-RA-767.

Zuckerman, R., Schmidt, G. J., & Dacko, S. M. (1982). Rhodopsin-to-metarhodopsin II transition triggers amplified changes in cytosol ATP and ADP in intact retinal rod outer segments. *Proceedings of the National Academy of Sciences of the United States of America, 79*, 6414–6418.